Uphill acceleration in a spatially modulated electrostatic field particle accelerator

I. Almansa*,[1] D. A. Burton†,[2] R. A. Cairns‡,[3] S. Marini§,[4] E. Peter¶,[1] F.B. Rizzato**,[1] and F. Russman††[1]

[1]*Instituto de Física, Universidade Federal do Rio Grande do Sul, Caixa Postal 15051, 91501-970 Porto Alegre, RS, Brasil.*
[2]*Department of Physics, Lancaster University, Lancaster, LA1 4YB, UK.*
[3]*School of Mathematics and Statistics, University of St Andrews, St Andrews, KY16 9SS, UK.*
[4]*LULI, Sorbonne Université, CNRS, École Polytechnique, CEA, Université Paris-Saclay, F-75252 Paris cedex 05, France.*

Spatially modulated electrostatic fields can be designed to efficiently accelerate particles by exploring the relations between the amplitude, the phase velocity, the shape of the potential and the initial velocity of the particle. The acceleration process occurs when the value of the velocity excursions of the particle surpass the phase velocity of the carrier, as a resonant mechanism. The ponderomotive approximation based on the Lagrangian average is usually applied in this kind of system in non accelerating regimes. The mean dynamics of the particle is well described by this approximation far from resonance. However, the approximation fails to predict some interesting features of the model near resonance, such as the uphill acceleration phenomenon. A canonical perturbation theory is more accurate in these conditions. In this work we compare the results from the Lagrangian average and from a canonical perturbation theory, focusing in regions where the results of these two approaches differ from each other.

I. INTRODUCTION

As laser intensity grows nowadays due to technological developments, new schemes of particle acceleration based on the ponderomotive potential and on laser-particle interactions are being applied, using the plasma as a medium or even the vacuum [1–4]. In recent papers [5, 6], it was shown that a particle could be accelerated by a spatially modulated electrostatic field. The acceleration mechanism takes place when the excursions of the particle velocity cross the line of the phase velocity of the carrier. At this moment, the particle is catapulted towards c − the speed of light. Beyond this promising result, the relatively simple physical model proposed in Refs. [5, 6] possesses some interesting features, which have not yet been properly explored.

One of these features occurs when the particle is near to the transition between reflecting and accelerating regimes. The closer to the accelerating regime, the more the particle is attracted by the resonance generated by the phase velocity of the carrier. If we look the phase-space of the particle (velocity against position) in this case, the particle is accelerated towards the phase velocity and then it is decelerated, being reflected by the field. This behaviour is known as uphill acceleration [7–9]. The uphill acceleration is also seen in laser produced plasmas, and can be understood as the acceleration the electrons feel which pushes them into the direction of growing field strength [10].

The mean dynamics of the particle can be described by variational techniques [11] or by an analytical Lagrangian approach [8] when the velocity excursions are far from resonance. However, the Lagrangian approach fails to predict, for example, uphill acceleration. According to Ref. [8], any averaged Lagrangian quadratic in the electric field has a unique value of the field amplitude corresponding to each value of the velocity. It implies the velocity is a monotonic function of the position which prohibits the presence of the uphill.

In this work, we present a canonical perturbation theory based on a change of coordinates in the Hamiltonian which describes the mean dynamics for non accelerating conditions of the particle and deals with the uphill acceleration. The paper is organized as follows: in Sec. II the physical model and the equations of motion of the particle are given, as well as the Lagrangian and the Hamiltonian approximations; in Sec. III the results are presented; and, finally, in Sec. IV we draw our conclusions.

II. THE MODEL

A. Full model

The one-dimensional model used in this work is exactly the same used in Ref. [5], where the dynamics of a single relativistic particle is determined by an electrostatic modulated wave. The Lagrangian of this system is written as

*ivanessa.almansa@ufrgs.br
†d.burton@lancaster.ac.uk
‡rac@st-andrews.ac.uk
§marini@ufrgs.br
¶peterpeter@uol.com.br
**rizzato@if.ufrgs.br
††russman@ufrgs.br

$$L = -mc^2\sqrt{1-\frac{\dot{x}^2}{c^2}} - q\varphi\left(x,t\right), \tag{1}$$

where c is the speed of light, φ is the electrostatic modulated wave potential and m and q are the mass and the charge of the electron, respectively.

The electrostatic modulated wave is expressed as

$$\varphi\left(x,t\right) = \varphi_0 \exp\left(-\frac{x^2}{\sigma^2}\right)\cos\left(kx-\omega t\right), \tag{2}$$

where the amplitude φ_0 is constant, k and ω are the wavevector and the frequency, respectively, of a carrier moving along the x axis, and σ measures the envelope length of the wave. We consider $\sigma \gg 1/k$ to enforce the condition of a slowly modulated wave train. The physics of this purely electrostatic modulated wave proposed here is similar to the physics of a particle submitted to the combined action of collinear electromagnetic and wiggler fields. This kind of arrangement is usually seen in inverse free-electron lasers devices [12–14].

The Hamiltonian which describes the evolution of the particle dynamics can be written as

$$H = \sqrt{p^2c^2 + m^2c^4} + q\varphi\left(x,t\right). \tag{3}$$

As seen in Refs. [5, 6], there are three different possible behaviours for the particle submitted to this Hamiltonian: either the particle is reflected by the electrostatic potential; or the particle passes through the potential with no appreciable change in its velocity; or the particle is accelerated by the potential. The particle is accelerated when, at some point during its path, its velocity is equal to or bigger than the phase velocity of the carrier.

B. Ponderomotive Approximation - *via* Lagrangian average

One way to describe the mean dynamics of the particle is using the ponderomotive approximation *via* the Lagrangian average, based on Refs. [7–9, 15]. This approximation may be used far from resonance and may be applied to estimate whether a transition of regimes occurs.

The Lagrangian average is written as

$$\mathcal{L} = \langle L\rangle = \left\langle \frac{-mc^2}{\gamma} - q\varphi\left(x,t\right)\right\rangle. \tag{4}$$

The velocity v of the particle may be expressed as $v = V + \delta\dot{x}$, where $\langle\delta\dot{x}\rangle = 0$ and $\langle\delta\dot{x}^2\rangle = \frac{q^2\varphi^2(x)}{2m^2{\gamma_0}^6\xi^2}$, where $\varphi(x) = \varphi_0\exp\left(-\frac{x^2}{\sigma^2}\right)$ is the envelope, with $\xi^2 = \omega^2\left(1-V/c\right)^2$ (V is the mean velocity of the particle). The kinetic term of the Lagrangian average is expressed as

$$\left\langle \frac{-mc^2}{\gamma}\right\rangle = -\frac{mc^2}{\gamma_0} + \frac{m}{2}{\gamma_0}^3\left\langle\delta\dot{x}^2\right\rangle, \tag{5}$$

where ${\gamma_0}^{-2} = 1-\alpha V^2/c^2$, with $\alpha = \omega^2/k^2c^2$.

This way, the Lagrangian average is simplified and after some algebra is finally written as

$$\mathcal{L} = -\frac{mc^2}{\gamma_0} - \frac{q^2}{4m}\frac{\varphi^2(x)}{\xi^2{\gamma_0}^3}. \tag{6}$$

Through the Lagrangian of Eq. (6) it is possible to find the equations that describe the mean dynamics of the particle far from resonance by using the Euler-Lagrange equations.

C. Canonical Perturbation Theory

Sufficiently far from resonance, as shown in Ref [5], the mean dynamics of the particle is well described by a canonical perturbation theory obtained *via* a change in coordinates in the Hamiltonian. The transformed Hamiltonian removes the high-frequency variables of the Hamiltonian of Eq. (3) and allows us to describe the dynamics solely in terms of new quantities [17]. These quantities form a self-consistent set of low-frequency variables.

Consider the Hamiltonian of Eq. (3), now designating it as $\mathcal{H}(x,p,t)$. Hamilton's equations are

$$\frac{dx}{dt} = \partial_p\mathcal{H}, \quad \frac{dp}{dt} = -\partial_x\mathcal{H}, \tag{7}$$

and are obtained from stationary variations of the action

$$S[C] = \int_C \left(p\,dx - \mathcal{H}\,dt\right) \tag{8}$$

with respect to the curve C, which has components $(x(t),p(t),t)$ on 3-dimensional extended phase space. It can be shown [16] that if (X,P) is related to (x,p) by a t-dependent canonical transformation, then the differential

$$\Omega = p\,dx - \mathcal{H}\,dt \tag{9}$$

on 3-dimensional extended phase space can be expressed as

$$\Omega = P\,dX - K\,dt + d\beta \tag{10}$$

where K is the Hamiltonian in (X,P,t) coordinates. Introducing the choice $\beta = f - P\partial_P f$ in Eq. (10), with $f = f(x,P,t)$, and substituting Ω using Eq. (9) gives

$$P\,d(X-\partial_P f) - K\,dt = (p-\partial_x f)dx - (\mathcal{H}+\partial_t f)dt. \tag{11}$$

Hence, the relationships

$$x = X - \partial_P f, \quad P = p - \partial_x f, \quad K = \mathcal{H} + \partial_t f \tag{12}$$

between the coordinates, the Hamiltonians and the generating function f emerge.

The potential of interest,

$$\varphi(x,t) = \varphi(x)\cos(kx - \omega t), \tag{13}$$

is that of a harmonic travelling electric wave, with angular frequency ω and wavenumber k, modulated by a slowly-varying amplitude $\varphi(x) = \varphi_0 \exp(-x^2/\sigma^2)$. The separation between fast and slow (or short and long) scales facilitates a perturbative analysis whose result can be interpreted as the motion averaged over one cycle of the fast oscillations. However, unlike in the Lagrangian approach, oscillatory terms are absorbed into a coordinate transformation instead of being averaged away. For simplicity, we will assume that the pointwise dependence of the amplitude is negligible up to second order in the perturbation theory.

The coordinate system (X, P) is adapted to the cycle-averaged motion, order-by-order in the perturbation theory, by transferring the explicit dependence on time t from the Hamiltonian $\mathcal{H}$ to the generating function f. The ensuing analysis is facilitated by introducing a parameter ϵ for tracking the perturbative order of terms. The parameter ϵ is merely a mathematical device with no physical meaning; it will be discarded at the end of the analysis.

Using (12), the Hamiltonian for the cycle-averaged motion is given by

$$K^\epsilon(X,P,t) = \mathcal{H}(X - \partial_P f^\epsilon, P + \partial_{x^\epsilon} f^\epsilon, t) + \partial_t f^\epsilon \tag{14}$$

where the superscript ϵ denotes a quantity with an explicit dependence on ϵ. Note that x^ϵ must be determined order-by-order from the implicit equation $x^\epsilon = X - \partial_P f^\epsilon$ where

$$f^\epsilon(x^\epsilon,P,t) = \epsilon f_1(x^\epsilon,P,t) + \frac{1}{2}\epsilon^2 f_2(x^\epsilon,P,t) + \mathcal{O}(\epsilon^3), \tag{15}$$

with each coefficient labelled by the corresponding power of ϵ. The choice $\varphi^\epsilon(x^\epsilon) = \epsilon\varphi_1(x^\epsilon)$ for the slowly-varying amplitude allows $f^\epsilon(x^\epsilon, P, t)$ to be determined order-by-order in ϵ using Eq. (14). The t-dependence of the coefficients in Eq. (15) are chosen to ensure the overall t-independence of the right-hand side of Eq. (14) to $\mathcal{O}(\epsilon^3)$.

The first three terms in the expansion

$$K^\epsilon(X,P,t) = K_0(X,P) + \epsilon K_1(X,P) + \frac{1}{2}\epsilon^2 K_2(X,P) + \mathcal{O}(\epsilon^3) \tag{16}$$

are

$$K_0(X,P) = \sqrt{P^2c^2 + m^2c^4}, \tag{17}$$

$$K_1(X,P) = \frac{c^2 P \partial_X \hat{f}_1}{\sqrt{P^2c^2 + m^2c^4}} + q\varphi_1(X,t) + \partial_t \hat{f}_1, \tag{18}$$

$$\begin{aligned} K_2(X,P) = {} & \frac{c^2(\partial_X \hat{f}_2 - 2\partial_P \hat{f}_1 \partial_X^2 \hat{f}_1)P + c^2(\partial_X \hat{f}_1)^2}{\sqrt{P^2c^2 + m^2c^4}} \\ & - \frac{c^4 P^2 (\partial_X \hat{f}_1)^2}{(P^2c^2 + m^2c^4)^{3/2}} \\ & - 2q\partial_P \hat{f}_1 \partial_X \varphi_1(X,t) - 2\partial_P \hat{f}_1 \partial_X \partial_t \hat{f}_1 + \partial_t \hat{f}_2. \end{aligned} \tag{19}$$

where $\varphi_1(X,t) = \varphi_1 \cos(kX - \omega t)$ and a circumflex indicates evaluation at $\epsilon = 0$, e.g. $\hat{f}_1 = f_1(X,P,t)$. Contributions arising from derivatives of the amplitude φ are assumed to be $\mathcal{O}(\epsilon^3)$.

Inspection of Eq. (18), Eq. (19) shows $\hat{f}_1$, $\hat{f}_2$ can be chosen to absorb all of the harmonic behaviour of the right-hand sides of Eq. (18), Eq. (19), respectively, without incurring secular behaviour in t. In particular, Eq. (18) leads to

$$\hat{f}_1 = \frac{q\varphi_1(X)\sqrt{P^2c^2 + m^2c^4}}{\omega\sqrt{P^2c^2 + m^2c^4} - Pkc^2} \sin(kX - \omega t) \tag{20}$$

and $\hat{f}_2 \propto \cos(2kX - 2\omega t)$ follows using Eq. (19), Eq. (20), where the coefficient of proportionality is independent of t. The remaining terms are independent of t and yield

$$K_1(X,P) = 0, \tag{21}$$

$$K_2(X,P) = \frac{m^2c^6k^2q^2\varphi_1^2(X)}{2(\omega\sqrt{P^2c^2 + m^2c^4} - Pkc^2)^2\sqrt{P^2c^2 + m^2c^4}}. \tag{22}$$

The Hamiltonian $\mathcal{K}(X,P) = K_0(X,P) + K_1(X,P) + K_2(X,P)/2$ describes the cycle-averaged motion of the particle in the lowest order approximation. Collecting Eqs. (17), (21), (22) gives

$$\begin{aligned} \mathcal{K}(X,P) = {} & \sqrt{P^2c^2 + m^2c^4} + \\ & \frac{m^2c^6k^2q^2\varphi^2(X)}{4(\omega\sqrt{P^2c^2 + m^2c^4} - Pkc^2)^2\sqrt{P^2c^2 + m^2c^4}}. \end{aligned} \tag{23}$$

The Hamiltonian of Eq. (23) describes the mean dynamics of the original Hamiltonian.

D. Normalization of the equations

For numerical reasons, it is useful to express the equations to be solved in a dimensionless way. In this section, we present the normalized forms of the equations used in this work.

The normalized Hamiltonian of the full system, corresponding to Eq. (3) is written as

$$H = \gamma + \varphi_0 \exp\left(-\frac{x^2}{\sigma^2}\right)\cos(x - t). \tag{24}$$

The relativistic factor $\gamma = \sqrt{[1 + p^2/\alpha]}$ is written in terms of the dimensionless momentum p, with $\alpha = v_\phi^2/c^2$ and $v_\phi = \omega/k$ being the phase-velocity of the carrier. The Hamiltonian H is normalized by the factor mc^2, while x, t, v, σ, p and φ_0 are substituted by x/k, t/ω, $v/\sqrt{\alpha}$, σ/k, pmc^2/v_ϕ and $\varphi_0 mc^2/q$, respectively.

Hamiltonian's canonical equations for Eq. (24) yield

$$\dot{x} = \frac{p}{\sqrt{\alpha^2 + \alpha p^2}}, \tag{25}$$

and

$$\dot{p} = \varphi_0 \exp\left(-\frac{x^2}{\sigma^2}\right)\left[\frac{2x}{\sigma^2}\cos(x-t) + \sin(x-t)\right]. \quad (26)$$

As can be seen in Eq. (25), the particle's velocity is an increasing function of momentum. Analyzing Eq. (26), as the value of $|x|$ decreases, the exponential factor goes to 1 and the term involving the cosine goes to 0. In this case, the dominant temporal term of Eq. (26) is $\varphi_0 \sin(x-t)$.

The Lagrangian of Eq. (6) can be normalized as well, taking the form (with $\xi = (1-V)$, being V normalized by $c/\sqrt{\alpha}$)

$$\mathcal{L} = -\frac{1}{\gamma_0} - \frac{1}{4\alpha}\frac{\varphi^2(x)}{\xi^2{\gamma_0}^3}. \quad (27)$$

Finally, Eq. (23), obtained from the canonical perturbation theory, is written as

$$\mathcal{K} = \Gamma + \frac{\alpha\varphi^2(X)}{4\big(P-\alpha\Gamma\big)^2\Gamma} \quad (28)$$

where

$$\Gamma = \sqrt{1+P^2/\alpha}. \quad (29)$$

From Eq. (28) it can be seen that asymptotically $K \approx \Gamma$ (because φ goes to zero for $X \gg \sigma$). So the velocity of the particle in the limit $X \to \infty$ tends to a constant. Additionally, Eq. (28) is equal to the ponderomotive Hamiltonian obtained in Ref. [5].

It is important to state that if one keeps the particle velocity away from resonance, $\partial\Phi/\partial V$ (where Φ is the ponderomotive potential for the respective approaches) is finite, ΔP (the variation of the momentum $\Delta P = P(t) - P(t=0)$) is small, and the Lagrangian average and the canonical perturbation theory are approximately identical.

However, closer to the resonance, the term $\partial\Phi/\partial V$ of the Lagrangian average diverges, while in the canonical perturbation theory this term is finite. P/Γ is not simply the velocity of the particle - the velocity is obtained from $V = \partial\mathcal{H}/\partial P$. It leads to different results near the acceleration regime, as it will be shown later.

III. RESULTS

As can be seen in Eq. (2), for values of $|x|$ much higher than σ, the amplitude of the potential goes to zero and the velocity is essentially constant. To run the simulations, the particle starts with $v_0 > 0$ and $x(t=0) = -3.5\sigma$. The simulations are stopped as soon as the particle reaches $x(t) = -3.5\sigma$ (with negative velocity) or $x(t) = 3.5\sigma$ and the velocity of the particle at this moment is taken as the final velocity (or exiting velocity).

The system analysed here has at least three different regimes, depending on the exiting velocity of the particle (which is denoted by the colour graded map of Fig. 1 - built for $\sqrt{\alpha} = 0.95$ and $\sigma = 100$), exactly as shown in Ref. [5]. The gray colour represents the reflecting regime. In this regime, the particle sees the electrostatic wave (as a barrier) and it is reflected by the field. The magnitude of the initial and the final velocities of the particle are exactly the same, but in the opposite direction. The passing regime is represented by the colour red. In the passing regime, the particle passes through the electrostatic potential, undergoing longitudinal jittering, but its final velocity is equal to the initial velocity.

Finally, there is what is called the accelerating regime. In this regime, the velocity excursions of the particle cross the line of the phase velocity of the wave (in this case, the Lagrangian average diverges, once ξ goes to zero, while the canonical perturbation theory does not). As soon as the line is crossed, the particle is accelerated towards the speed of light. The final velocity of the particle is indicated through the colours yellow, green and blue. There are small regions in the accelerating regime that resemble half moons, in which the acceleration mechanism is not effective. At the corner of these half moons, the entering and the exiting velocities of the particle are exactly the same (this is analogous to a fixed point).

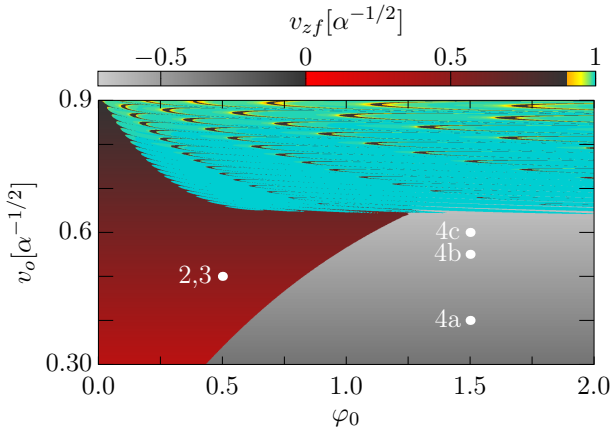

FIG. 1: Colour graded map for $\sqrt{\alpha} = 0.95$ and $\sigma = 100$. The colors represent the final velocity of the particle.

The labeled points of Fig. 1 are explored in details in the following figures.

Fig. 2 (for $v_0 = 0.5$, $\varphi_0 = 0.5$, $\sigma = 100$ and $\sqrt{\alpha} = 0.95$) shows that the time evolution of the particle in panel (a) and the phase-space v *vs.* x in panel (b). The solid line represents the solution obtained through the integration of Eqs. (25) and (26), while the dashed line is the phase velocity of the wave and the thick red solid line is the time-averaged value of the dynamics of the particle. To obtain the red solid line, we evaluate the mean value of the time, position and velocity between two consecutive

peaks of velocity. As a result, this approach provides a smoother curve in comparison to fixed or moving window averaging techniques.

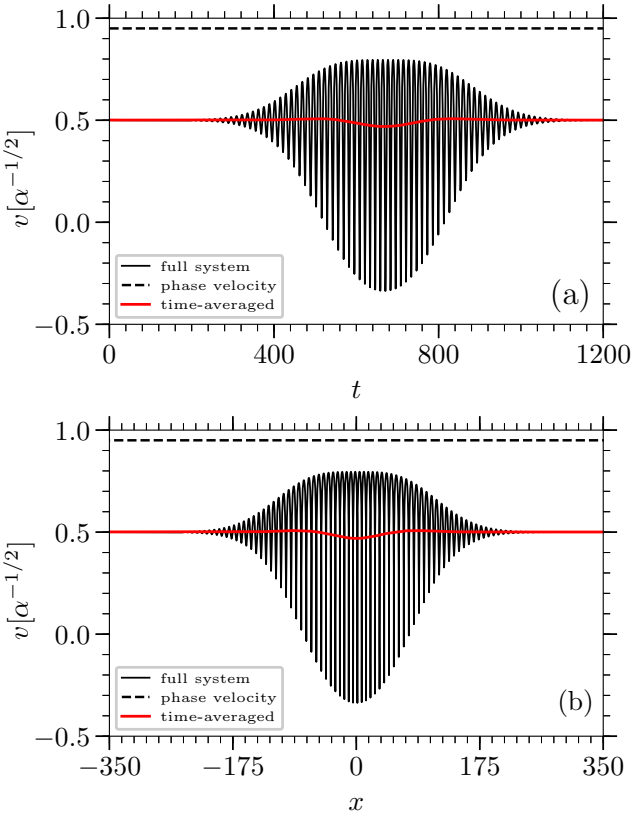

FIG. 2: The time evolution of the velocity of the particle is plotted in panel (a), while panel (b) shows the phase-space of the particle dynamics for $\varphi_0 = 0.50$, $v_0 = 0.50$, $\sigma = 100$ and $\sqrt{\alpha} = 0.95$. The red solid line is the mean dynamics of the particle.

Far from resonance, the canonical perturbation theory well describes the mean particle dynamics both in passing or in reflecting regimes. Fig. 3 shows the phase-space of the particle. The red solid line is the time-averaged dynamics of the particle from the integration of the Eqs. (25) and (26), the blue solid line is obtained from the canonical perturbation theory for the Hamiltonian (Eq. (28)) and the green solid line is obtained from the Lagrangian average (Eq. (27)). It is important to notice that the initial and final velocities are the same. As $x \to -\infty$ and $x \to +\infty$, the field vanishes and only the kinetic energy of the particle remains. The blue and red curves reasonably agree. However, the green line is considerably different: to the lowest approximation, the energy expression $E = V\partial\mathcal{L}/\partial V - \mathcal{L}$ derived from the Lagrangian of Eq. (27) monotonically associates a unique field intensity to a given velocity - it means that there is a unique value of $\varphi(x)$ corresponding to any value of the velocity [8]. This association gives incorrect results.

When the system is near resonance, new features appear in the dynamics of the particle. The case of the

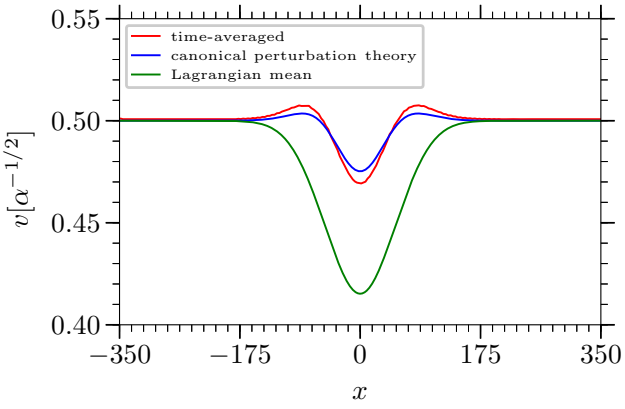

FIG. 3: Phase-space for $v_0 = 0.50$, $\varphi_0 = 0.50$, $\sigma = 100$ and $\sqrt{\alpha} = 0.95$. The red solid line is the mean dynamics obtained from Eqs. (25) and (26). The green (blue) solid line is from the Lagrangian (Hamiltonian) approximation.

reflecting regime, shown in Fig. 4, is of particular interest, where the solid red line represents the mean obtained through the integration of the Eqs. (25) and (26), while the blue and the green solid lines are the results from the canonical perturbation theory and the ponderomotive approximation *via* Lagrangian average, respectively. Far from resonance, the oscillations of the particle are symmetrical. This way, the phase-space of the particle is described by horizontal lines ($+v_0$ and $-v_0$) connected by a transition curve, as can be seen in panel (a), for $\varphi_0 = 1.5$ and $v_0 = 0.4$. All the curves agree reasonably.

As we increase the initial velocity, the excursions of the velocity of the particle come closer to the resonant velocity, breaking the symmetry of the oscillations: the particle spends more time at higher velocities (pushing the time-averaged results of the full simulations to higher values). This effect, known as uphill acceleration, induces the appearance of the knob shown by the solid red line (from the full system) in panels (b) and (c) of Fig. 4. The phase velocity line acts as an attractor of the particle but it is still unable to accelerate the particle. As in panel (a), the blue and green solid lines are from the canonical perturbation theory of the Hamiltonian and from the Lagrangian average ponderomotive approximation.

A qualitative difference between the curves can be seen in panels (b) and (c) (built for $\varphi_0 = 1.5$ and for $v_0 = 0.55$ and $v_0 = 0.6$, respectively). While the canonical theory based on the Hamiltonian reproduces the uphill acceleration, the approximation *via* the Lagrangian average does not. The reason is that the particle cannot possess the same value of its velocity at positions with different field amplitudes [8] - it also explains the difference observed in Fig. 3. Here, the direct relations between velocity, position and field amplitude do not allow the uphill acceleration. In the case of the approximation *via* the canonical perturbation theory, the relations depend on the momentum, which has a more complicated connection with the velocity, allowing the same value of velocity for different

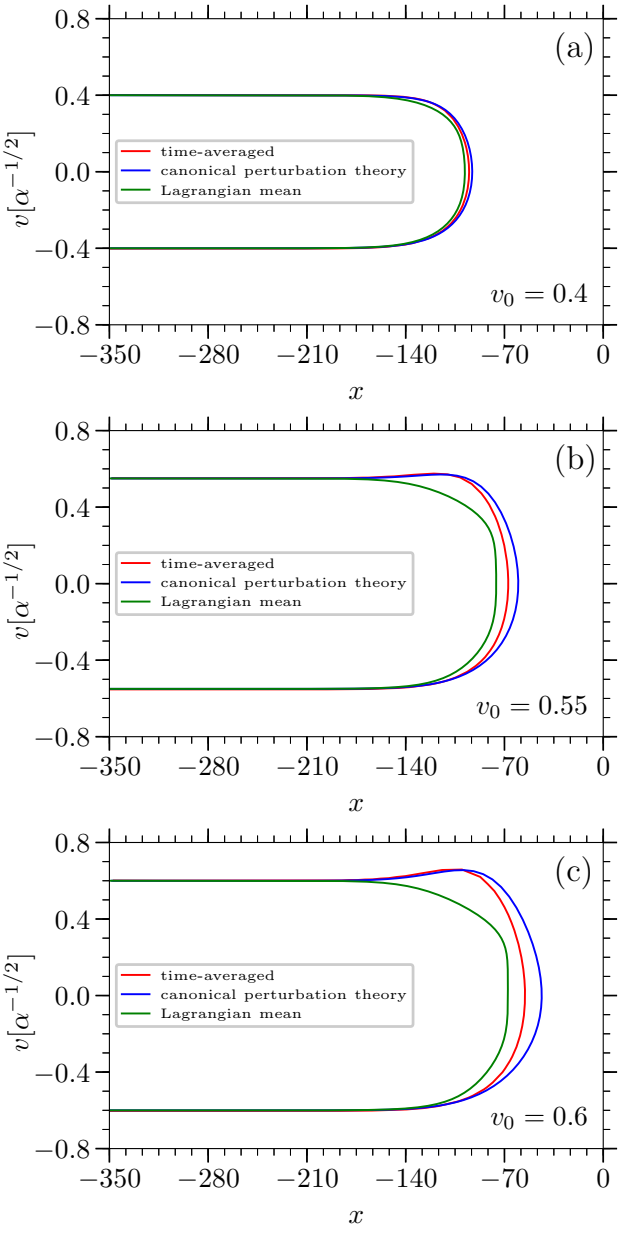

FIG. 4: Phase-space for $\varphi_0 = 1.5$, $\sigma = 100$, $\sqrt{\alpha} = 0.95$ and for panel (a) $v_0 = 0.40$, panel (b) $v_0 = 0.55$ and panel (c) $v_0 = 0.60$.

positions with different values of the field amplitude. Additionally, the curve of the ponderomotive approximation *via* the Lagrangian average cannot be used for parameters near the transition to the accelerating regime. The existence of ξ^2 in the Lagrangian average of Eq. (27) introduces a singularity which occurs when the particle is about to be accelerated. **However, even though the ponderomotive approximation, itself, fails at resonance, it can describe the beginning of the acceleration process.**

IV. CONCLUSION

In this work, we compared the exact solutions obtained from the model described by the Hamiltonian of Eq. (3) to the solutions of the ponderomotive approximation *via* Lagrangian average and the canonical perturbation theory. Far from resonance, the approximations well describe the dynamics of the system, in the reflecting regime.

However, as the system comes closer to the resonance in the reflecting regime, the approximation based on the Lagrangian average strays from the exact solution. The approximation cannot depict, for example, the uphill acceleration. Furthermore, the approximation fails to predict the two peaks present in the mean dynamics of the passing regime. In both cases, the exact solution associates the same velocity with different positions and field intensities, which cannot be accounted by the lowest order Lagrangian approach [8].

On the other hand, the canonical perturbation theory allows us to predict the mean dynamics in both regimes including the uphill acceleration and the two peaks of the passing regime. In the Hamiltonian approach one works more formally with momentum dependent generating functions and velocities are obtained accordingly. This approximation will be explored **(focusing in different scenarios, including finite cross sections for the envelope, multi-dimensional analysis and using different shapes for the envelope)** and applied to other systems, in upcoming works.

Acknowledgments:
We acknowledge support from CNPq and CAPES, Brasil, and from AFOSR, USA, under research grant FA9550-16-1-0280. S.M. acknowledges support from Grant No. ANR-11-IDEX-0004-02 Plas@Par. D.A.B. and R.A.C. are supported by the UK Science and Engineering Research Council grant EP/N028694/1. We thank the referee for their useful suggestions.

[1] D. Lin, Q. Kong, Z. Chen, P. X. Wang and Y. K. Ho, J. Phys. D: Appl. Phys. **41**, 135107 (2008).
[2] E. A. Startsev and C. J. McKinstrie, Phys. Rev. E **55**, 7527 (1997).
[3] D. E. Ruiz, C. L. Ellison, and I. Y. Dodin, Phys. Rev. A **92**, 062124 (2015).
[4] D. Patil and M. V. Takale, Laser Phys. Lett. **10**, 115402 (2013).
[5] S. Marini, E. Peter, G. I. de Oliveira and F. B. Rizzato, Phys. Plasmas **24**, 093113 (2017).
[6] F. Russman, S. Marini, E. Peter, G. I. de Oliveira and F. B. Rizzato, Phys. Plasmas **25**, 023110 (2018).

[7] D. Bauer, P. Mulser and W.-H. Steeb, Phys. Rev. Lett. **75**, 4622 (1995).
[8] D. A. Burton, R. A. Cairns, B. Ersfeld, A. Noble, S. Yoffe, D. A. Jaroszynski, Proc. SPIE 10234, Relativistic Plasma Waves and Particle Beams as Coherent and Incoherent Radiation Sources II, 102340G (2017); doi: 10.1117/12.2270542
[9] R. A. Cairns, D. A. Burton, B. Ersfeld, A. Noble, S. R. Yoffe, and D. A. Jaroszynski, Ponderomotive force in a travelling wave. In: European Physical Society Conference on Plasma Physics, 2017-06-262017-06-30.
[10] H. Ruhl, Phys. Plasmas **3**, 3129 (1996).
[11] R. G. Littlejohn, J. Plasma Physics **29**, 111 (1983).
[12] A. van Steenbergen, J. Gallardo, J. Sandweiss, and J.-M. Fang, Phys. Rev. Lett. **77**, 2690 (1996).
[13] L. F. Monteiro, A. Serbeto, K. H. Tsui, J. T. Mendonça, and R. M. O. Galvão, Phys. Plasmas **20**, 073101 (2013).
[14] E. Peter, A. Endler, and F. B. Rizzato, Phys. Plasmas **21**, 113104 (2014).
[15] I. Y. Dodin and N. J. Fisch, Phys. Rev. E **77**, 036402 (2008).
[16] V. I. Arnold, *Mathematical Methods of Classical Mechanics*, 2nd ed., Springer-Verlag, (1989).
[17] C. Grebogi and R. G. Littlejohn, Phys. Fluids **27**, 1996 (1984).
[18] D. E. Ruiz and I. Y. Dodin, Phys. Rev. A **95**, 032114 (2017).